Modeling of Chloride Concentration Effect on Reinforcement Corrosion

Dita Vořechovská* & Jan Podroužek

*Brno University of Technology, Faculty of Civil Engineering, Institute of Structural Mechanics,
Veveří 95, 602 00 Brno, Czech Republic*

&

Markéta Chromá, Pavla Rovnaníková & Břetislav Teplý

*Brno University of Technology, Faculty of Civil Engineering, Institute of Chemistry,
Žižkova 17, 602 00 Brno, Czech Republic*

Abstract: *The corrosion of reinforcement is one of the major causes of deterioration of reinforced concrete (RC) structures, considerably affecting their durability and reliability. The rate of reinforcement corrosion is governed by, among other factors, the presence of chlorides on the surface of the steel. The assessment of such deteriorating effects necessitates the development of relevant models and the utilization of advanced simulation techniques to enable the probabilistic analysis of concrete structures. In this article an approach for the assessment of the durability and reliability of RC structures under attack from chlorides is introduced. The field of chloride concentration at different locations in the structure (represented in 2D space by chosen longitudinal or cross sections) is modeled as a function of time by a cellular automata (CA) technique. The results of this simulation are then utilized for the assessment of a steel corrosion prognosis using a probabilistic 1D model at chosen points, although the rate of corrosion is based on experimental results. The concentrations of chlorides and pH levels are reflected in this way. The described approach is applied to an illustrative example showing the feasibility of capturing the effect of chloride concentration on the steel* corrosion rate and consequently on the assessment of the service life and/or reliability of the structure.

1 INTRODUCTION

Damage due to reinforcement corrosion is recognized as one of the major causes of deterioration of reinforced concrete structures, with service life reduction as a consequence. Reinforcement concrete durability is then determined by its resistance against various chemical and physical processes. An extensive amount of research on this topic has been organized and reported over the last decades. It has been observed that many of the problems associated with corrosion can be attributed to the presence of salts (e.g., see Bogard et al., 1990).

Among the key factors influencing reinforcement corrosion in concrete are the presence of moisture and the ingress of oxygen from the air. Concrete exposed to the outside climate usually contains enough moisture required for the corrosion process, and the concrete cover enables the penetration of a sufficient amount of oxygen (Nürnberger, 1984; Schueremans et al., 2007). Less permeable and thicker concrete cover prolongs the time to corrosion initiation, and hence the service life of reinforced concrete structures. Thus, concrete quality (e.g.,

*To whom correspondence should be addressed. E-mail: *vorechovska.
d@fce.vutbr.cz.*

pore structure and the presence of cracks) plays a decisive role.

The other important factors also influencing the rate of corrosion of steel bars in concrete include relative humidity (RILEM, 1996), rainfall (So and Millard, 2007), and temperature (So and Millard, 2007; Jensen et al., 1999; Nguyen et al., 2006). The corrosion rate is likewise significantly influenced by the presence of chloride ions (Karimi and Ramachandran, 2000).

When chlorides are present in RC structures, the rate of their penetration into concrete and their concentration may play a significant role for the corrosion process. This should be reflected when designing or assessing a concrete structure with consideration of the durability issue. The effect of chloride concentration on corrosion rate has also been the focus of our experiments, which are partially presented in this article. Corrosion may be initiated by chloride contamination when the chloride concentration in the vicinity of reinforcement exceeds a certain (critical) value. Once the corrosion of reinforcement starts, several degradation events may be encountered (propagation period). These are primarily concrete cracking, spalling of concrete cover, a decrease in the effective cross-section area of reinforcement, and/or the reduction of bond between reinforcing bars and concrete.

These degradation phenomena have to be considered when designing/assessing RC structures as the application of design for durability may bring pronounced economical and sustainability impacts. Unfortunately, the prescriptive approach of current standards (e.g., Eurocodes EN 1990 and EN 1992) does not directly allow a design method focused on a specific (target) service life and/or a specific level of reliability. This would require the consideration of inherent uncertainties in material, technological, and environmental characteristics to be dealt with while assessing the service life of a structure. To respect this, a probabilistic approach should be utilized as was frequently applied previously (e.g., Stewart and Rosowsky, 1998); such an approach is also incorporated in new standard documents (*fib* Model Code and ISO 13823) and in the present article. The service life of a building or structure is determined by its design, construction, aging, and maintenance during use. The combined effect of both structural performance and aging should be considered wherever relevant. The limit state (LS) approach is applicable and in general governed by the probability condition:

$$P_f = P[A(t) \geq B(t)] \leq P_d \qquad (1)$$

where P_d is design (required) probability, t is time, A is action effect, and B is barrier; both A and B (and hence the probability of failure P_f) are generally time dependent. This has not been considered in the cases of serviceability limit states (SLSs) or ultimate limit states (ULSs) in design practice very frequently up to now. The time t_S corresponding to the limit given by Equation (1), that is, the service life, and the deteriorating effect A are assessed by utilization of the appropriate degradation models and LS applying a probabilistic approach. Note that instead of the probability of failure P_f, the index of reliability β is alternatively (and rather frequently) utilized in practice (e.g., see ISO 2394 and EN 1990).

In the case of design for durability, a new category of LSs has recently been discussed called initiation or durability limit states (DLSs). This kind of limit state represents simplified LS intended to prevent the onset of deterioration. It is based on the initiation of deterioration (see also the documents *fib* Model Code and ISO 13823). Formally, DLSs fall into the group of SLS. For durability design these initiation LSs have to be combined often with other LS considering also the propagation period. The level of reliability in the context of durability should be left to the client's decision together with the definition of a target service life, creating in this way a necessary background for his/her critical decision (e.g., economical optimization).

The present article concentrates on modeling of reinforcement corrosion, the assessment of chloride concentration fields by numerical methods, and on their practical utilization while evaluating the limit states, service lives, and relevant reliability of reinforced concrete structures. Our presented experimental work shows the effect of chloride concentration and pH values on the rate of steel reinforcement corrosion. The development of the concentration of chlorides within the cross section of an RC structure is modeled by a specific cellular automata (CA) technique adopted from Biondini et al. (2004). The results of the CA technique and the laboratory experiments are applied in the assessment of steel effective area decrease due to corrosion using the model by Rodriguez et al. (1996), extended by the authors when considering chloride concentration and pH values. Also, the enhancement of the CA simulation technique to gain the spatial and temporal variations of Cl^- is demonstrated; in this way the parts of a structure where the level of chlorides exceeds the critical threshold concentration may be predicted and consequently utilized while assessing the initiation period—the depassivation of reinforcement. This may be done in a variety of concrete structures under different "loading" situations by salt application and the utilizing of several new types of boundary conditions; to facilitate such a practice the software tools have been developed. Finally, the introduced approach is applied to an illustrative example showing the effect of chloride concentration level at different points in an RC cross section on the rate of

steel corrosion in time and also the effect of seasonal de-icing salt application. Prevention of steel corrosion has to be already taken into account during the design stage. The presented approach may be exploited as a relatively simple design tool while designing a new concrete structure and thus enhance the possibility of exploring the limits of the materials and technologies in question under various conditions and help in decision-making procedures. However, currently the future expenses for maintenance and repair are often not taken into account.

2 STEEL CORROSION

In this section chemical and physical processes leading to corrosion initiation and propagation and the effect of the presence of chlorides on steel corrosion are briefly reviewed based on a survey of the literature. In the next, experimental work proposed by the authors of this article showing the effect of chloride concentration and pH level is presented.

2.1 Corrosion initiation, propagation, and chloride effects

In common concrete the reinforcement exists in an alkaline environment (pH > 12) with a high content of hydroxide ions (OH^-) originating from the dissociation of calcium hydroxide and likewise from the dissociation of sodium and/or potassium hydroxide. The calcium hydroxide is formed during the hydration of cement, and sodium or potassium hydroxide during the hydrolysis of minerals containing Na_2O or K_2O, respectively. Under these conditions the reinforcement surface is covered with a dense and effective adhesive protective layer with a thickness of approximately 10 nm (steel passivation) (Schueremans et al., 2007).

The corrosion of reinforcement embedded in concrete is an electrochemical process during which coupled anodic and cathodic reactions take place. This process has been described elsewhere (e.g., see Nürnberger, 1984, or Bentur et al., 1997). Generally, corrosion can begin due to the presence of oxygen and moisture when the passive film is destroyed (after reinforcement depassivation) by

(i) A decrease in the pH value of the pore solution to values below 9. Such a reduction in alkalinity is the result of the carbonation process, that is, of calcium hydroxide reactions with atmospheric CO_2 that diffuses through the concrete's pores. Its modeling and some consequences for RC structure durability are reported in numerous publications (e.g., see DuraCrete, 1998, or *fib* Model Code).

(ii) Chloride ion penetration when the chloride content of material in contact with reinforcement exceeds a critical (threshold) chloride concentration.

The chloride threshold concentration is preferably presented by means of the total amount of chloride by weight of cement, the amount of free chloride, the concentration ratio of free chloride ions to hydroxide ions or the ratio of acid-soluble chloride content, and the acid neutralization capacity (the content of acid needed to reduce the pH of concrete and cement paste suspended in water to a particular value) (Ann and Song, 2007). In terms of currently used representations, the total chloride content related to the cement weight is considered as the best alternative. This representation results in a reduction in the range of determined values of critical chloride concentration and represents the total potential aggressive ion content expressed relative to the total potential inhibitor content (Glass and Buenfeld, 1995, 1997; Duprat, 2007; Ann and Song, 2007).

One reason for the lack of agreement among the measured values of critical chloride concentration is the influence of several factors. The key factor was found to be the physical condition of the steel–concrete interface (Glass and Buenfeld, 1995; Ann and Song, 2007). Another reason is the differences among the methods of measurement of the chloride threshold concentration, the chloride content at the steel surface, and the time of onset of corrosion. The onset of corrosion may be detected by measuring half-cell potential, monitoring the macrocell current between an anode and a cathode, monitoring the corrosion rate measured by the polarization technique or AC impedance method (Montemor et al., 2003), or visual inspection as accepted by Bentur et al. (1997).

The value of 0.4% denoting chloride content by weight of cement is currently suggested as the chloride threshold concentration for buildings exposed to a European temperate climate, although 0.2% is for structures exposed to a more aggressive environment (Glass and Buenfeld, 1995; Duprat, 2007).

2.2 Experiments

In this section, experimental work focused on the corrosion resistance of steel reinforcement in the presence of chlorides is presented. The reinforcing bars used were made from steel No. 10425 according to Czech standard ČSN 425535. Steel bars with a diameter of 10 mm were cut to a length of 100 mm and an epoxide coating was applied on the cut faces. The steel specimens were weighed and placed into polyethylene flasks of
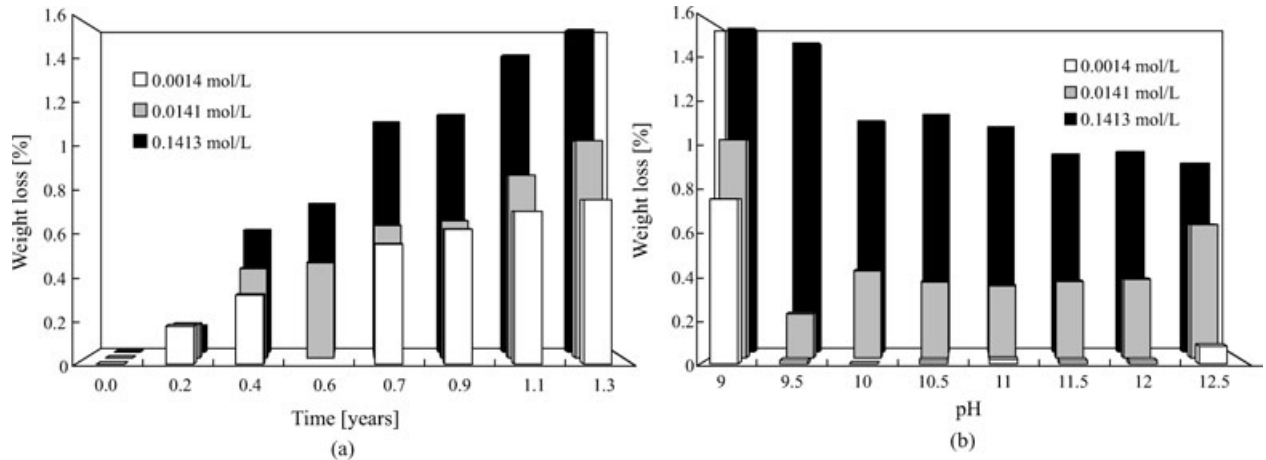
Fig. 1. Steel rebar weight loss: (a) over time for pH = 9; (b) for different pH values.

100 mL volume, filled with NaCl solution with different pH levels (ranging from 9 to 12.5, step 0.5) and three different chloride concentrations (0.0014, 0.0141, and 0.1413 mol/L).

The specimens were taken out of the flasks every 60 days, cleaned from corrosion products and weighed to determine the weight loss. Measurements of mass loss were carried out according to the ratio Cl^-/OH^-, which is utilized for assessment of corrosion environment quality (Bird et al., 1988). For pH value 9, the evolution of weight loss due to corrosion over time is shown in Figure 1a for three different chloride concentrations. The influence of Cl^- concentration is significant. The dependence of weight loss on the pH value over a time of 1.3 years obtained from experiments for three chloride concentrations is presented in Figure 1b. The pH value is clearly one of the factors influencing the chloride threshold concentration (see Section 4.2).

The loss in the rebar radius was calculated as a ratio of the weight loss to the specific weight of the rebar and the surface area. Due to the epoxide coating on the cut faces, the lengths of the rebar samples remain the same. In the calculations, for the sake of simplification it is assumed that the corrosion is uniform even though pitting corrosion was present. Subsequently, the corrosion rate is determined by dividing the loss in the rebar radius by the corresponding time. The corrosion rates have been found to be only slightly time dependent in the presented experiments. For the sake of simplicity, the values for $t = 1.3$ years were employed. The results of the corrosion rates for solutions with pH = 9 and 12.5 are presented in Table 1, showing the pronounced effect of Cl^- concentration.

This kind of simplified experiment differs from the conditions existing during the real (natural) behavior

Table 1
The corrosion rates for pH = 9 and 12.5

pH value	Cl⁻ (mol/L)	Corrosion rate (μm/year)
9	0.0014	14.56
	0.0141	19.98
	0.1413	30.80
12.5	0.0014	1.57
	0.0141	12.15
	0.1413	17.90

of reinforcement embedded in concrete; for example, the influence of relative humidity, temperature, and surrounding concrete were not taken into account. However, the results of the simplified experiment quantitatively reflect the loss of rebar due to corrosion in the presence of chlorides with different compositions of solutions. Thus, at least the trends for corrosion rate due to pH level and Cl^- concentrations may be captured in this way as it is shown in Section 4.2.

3 CHLORIDE PENETRATION: MODELING

The simulation of chloride concentration distribution over the concrete structure will be introduced in the following sections by

(a) application of analytical 1D models for chloride ingress into concrete;
(b) using the CA, which enables spatial and temporal estimation of the chloride penetration process (deterministic or stochastic alternative).

The conventional analytical 1D models serve here for certain comparisons and for finding the type of

boundary rule for the CA technique further used for numerical applications.

3.1 Analytical models

Several approaches exist for description of the time-dependent process of chloride ingress in concrete. Many models utilize the widely used Crank's solution to Fick's second law of diffusion probably first applied by Collepardi et al. (1972). This approach is based on the fact that observations indicate that the transport of chlorides in concrete is mainly diffusion controlled, and thus the convection zone is relatively small (Hunkeler, 2005). The solution is derived from the assumption that concrete is homogenous, initial chloride content C_0 is zero, surface chloride content $C_{S,0}$ is constant, chloride binding is linear, and the effect of coexisting ions is constant. The model in one-dimensional form reads:

$$C(x, t) = C_{S,0} \left[1 - \mathrm{erf} \left(\frac{x}{2\sqrt{D_a t}} \right) \right] \qquad (2)$$

where $C(x, t)$ is concentration of chlorides at depth x at the time of exposure t (usually $x = a$, where a is concrete cover) and D_a is the apparent diffusion coefficient. D_a and $C_{S,0}$ are estimated from field exposure or laboratory tests. The erf is the error function.

The problem of proper representation of D_a has been tackled on several levels of simplification. The presumption of D_a being constant in time and space is too conservative (Tang and Gulikers, 2007); nevertheless, for ordinary concrete without blended materials this simplification can be used (Duprat, 2007). Tikalsky (2005) overcomes this problem partially by using the statistics of a data set collected from the *in situ* measurements of chloride penetration from more than 230 bridge decks in the United States. The time-dependent diffusion coefficient $D(t)$ may also be calculated on the basis of the proposed formula (Tang and Nilsson, 1992; Thomas and Bamforth, 1999; Mangat and Molloy, 1994; *fib* Model Code); however, the proper mathematical derivation of $D(t)$ and comparison of possible errors caused by some oversimplified mathematical expressions were presented by Tang and Gulikers (2007).

Further, it has been found that the surface chloride concentration ($C_{S,0}$) increases with time (Nilsson, 2006; Tang and Gulikers, 2007; Costa and Appleton, 1999). Nevertheless, Duprat (2007) assumed that constant surface chloride content is a commonly accepted assumption in the case of structures exposed to de-icing salts, and that chlorides accumulate only in coastal zones.

Although the above-mentioned models based on an error function complement solution are widely used by engineers in practical applications due to their relatively simple mathematical expressions, the omission of chloride binding is a weakness of these models. However, although models based on actual physical or chemical processes would be more adequate, they are often only used for research purposes owing to the necessity for more involved types of calculations (e.g., see the model by Xi and Bažant, 1999, for chloride binding capacity and diffusivity calculations). Also, such complex models are more data demanding, which is usually a constraint during practical application. Only some models have been simplified into an engineer-friendly form (Papadakis et al., 1996; Tang, 2007).

The majority of the above-mentioned models were originally published as deterministic ones. As explained above, the probabilistic approach is believed to be more adequate—among other benefits such an approach enables one to execute a probability analysis as indicated by condition (1). This is reflected, for example, in *fib* Model Code where the limit conditions and the model for chloride diffusion are treated in this manner. Also, some other analytical models have already been converted into probabilistic form—about 20 such models were reported (Teplý et al., 2007); for single probabilistic models see, for example, Stewart and Rosowsky (1998), Tikalsky (2005), and Val et al. (2000). Moreover, the authors believe that the CA technique may serve as an effective tool for diffusion problem simulation (also encompassing a stochastic option); this is explained in the following section.

3.2 Cellular automata

A cellular automaton is a special class of evolutionary algorithm, which is a mathematical idealization of physical systems in which space and time are discrete (Wolfram, 1994). In principle, any physical system satisfying differential equations may be approximated as a cellular automaton by introducing discrete coordinates and variables, as well as discrete time steps. A cellular automaton consists of a collection of cells on a grid of specified shape that evolves through a number of discrete time steps according to a set of local rules based on the states of neighboring cells. The rules are then applied iteratively for as many time steps as desired. The overall simulation time is then the sum of all time steps.

The CA solution of the diffusion equation was adapted from Biondini et al. (2004). The construction is for our purposes represented by a 2D grid of regular uniform cells. Each cell has its own state value representing the component concentration (e.g., the chloride ions). The process of chloride ingress is governed by a local rule in which the evolutionary coefficients Φ_i ($i = 1, 2, 3, 4, 5$) assign the level of chloride concentration in adjoined cells—in horizontal and vertical

directions, that is, north, east, south, and west:

$$X_{(t+1)} = \Phi_1 X_t + \Phi_2 N_t + \Phi_3 E_t + \Phi_4 S_t + \Phi_5 W_t \quad (3)$$

where the discrete variables $\{X_t, N_t, E_t, S_t, W_t\}$ represent the concentration of the component in the given cell at time t. The values of the evolutionary coefficients Φ_i must verify the following normality rule:

$$\sum \Phi_i = 1 \quad (4)$$

as required by the mass conservation law applied to the amount of chloride in the cell and its neighborhood. The following relationship is mandatory for the whole grid of cells within each time step Δt:

$$D = \Phi_1 \Delta x^2 \Delta t^{-1} \quad (5)$$

where Δx represents the cell size, D is the diffusion coefficient, and Φ_1 is the chloride evolutionary coefficient. Note that the values of evolutionary coefficients are determined to define the level of redistribution within the given neighborhood (4 cells), for example, for the directionality effects in heterogeneous media. The speed of the diffusion is governed in Equation (5) by means of the diffusion coefficient D, so the sum of the values Φ_2, Φ_3, Φ_4, Φ_5, and the value Φ_1 should be in the ratio 1:1, which implies that in the 2D isotropic case the values Φ_2 to Φ_5 can only be 0.125 and $\Phi_1 = 0,5$.

One of the essential parts of the CA configuration is the boundary rule setting, or in other words the definition of the system's behavior in the areas where there is contact with the outer medium, that is, with a place beyond the simulation region. Several types of boundary rule may be used. The boundary type most suitable for comparison with the results of a conventional analytical 1D model (Papadakis et al., 1996) is the "reflecting boundary," rendering almost identical results in a geometry where component concentration at a certain point and at a certain time is affected only by propagation from one direction (this comparison is not presented within the scope of this article). Note that this approach to the boundary problem is suitable only for the case where it is supposed that the transported quantity does not leave the simulation region once it enters. This might be the case for chloride ions, although it is known that in reality there is some kind of back-propagation. It is a topic of the authors' ongoing research to appropriately define the boundary system interaction for different transport phenomenon; however, for the purpose of this work it was rational to use some degree of simplification when dealing with the task of boundary interaction.

To test and further exploit the proposed methodology, a deterministic and stochastic 2D C++ application featuring CA is being developed. While applying this code a grid of CA is created according to the initial parameters. The main parameters are the diffusion coefficient, cell size, time step, and the evolution coefficient—see Equation (5). After defining the aggressive environment (e.g., supply of chlorides from a de-icing salt application) the transformation process may begin. After each time step, a text file with the current system state is created. The whole process is displayed on the screen as a real-time graphical visualization. Proper interpretation of these results provides information about local changes in the structure (e.g., cross section) properties (chloride concentration) over time. An example is shown in Figure 2 where a visualization of the degradation evolution in a beam cross section is shown for the total times of 0, 5, 25, and 50 years. The colors from gray to black represent the state from zero to higher chloride concentration in cells.

The environmental impact, not necessarily invariant (in location, amount, and/or time), is expressed via boundary cells. These may change their state value over time, either periodically, by a specified function, or randomly. Also, the contact region may be subjected to differentiation by the use of various configurations within a particular time. In this manner it is possible to simulate various events, for example, the seasonal effect of de-icing salt application. It was presumed in this example that the salt feed occurs periodically for 22 years in
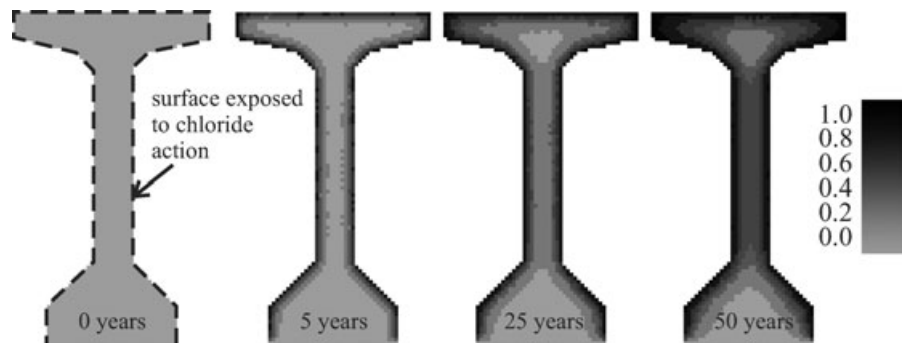
Fig. 2. Numerical example: AASHTO IV 711.2/1828.8 mm; cross-section degradation evolution visualization; 1871 cells of 20×20 mm; the interval $\langle 0; 1 \rangle$ represents the relative chloride concentration.
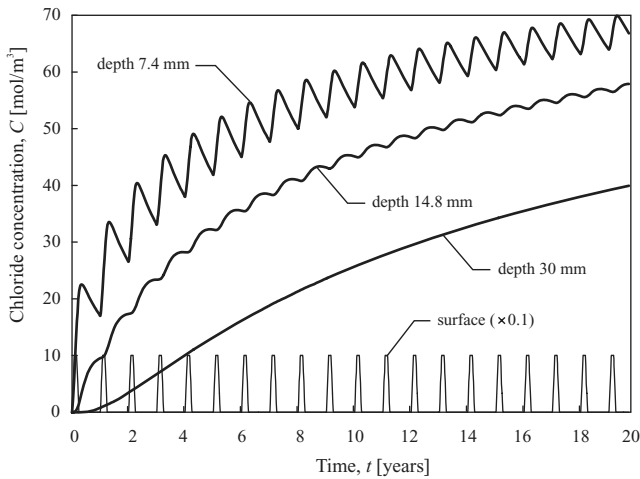
Fig. 3. The effect of seasonal de-icing salt application at different depths of concrete and the concentration on the surface (external salt feed), which is multiplied by 0.1.

the winter season (3 months a year). Figure 3 shows the periodic application of salt on a concrete surface and the resulting chloride concentrations at certain depths of concrete. It is not surprising that the concentration fluctuation over time is more obvious at the propagation surface and becomes less apparent with the depth of the specimen. It is also worth mentioning that the transport effect proceeds continually, even if there is currently no chloride feed, for example, in the summer. Effects as salt washing out during summer rain in the exposed parts of the structure can also be treated by CA (not executed in the present article). Moreover, the change in chloride permeability over time, for example, due to the use of nontraditional binders in concrete has been studied (Podroužek et al., 2008). Clearly, CA is an advanced soft-computing technique substituting for the direct solution of differential equations. Regarding CA as a numerical technique, the main advantage compared to conventional approaches is the versatility and transparency of the process and the possibility of effective parallel computation.

Stochastic effects may be dealt with as well, modifying the procedure by assuming the local values of the chloride field as well as the diffusion coefficient to be random values with a given probabilistic distribution function (PDF). To obtain statistics for a certain cell (e.g., for a critical point), software application can then be ran *n*-times while adjusting the input data and boundary conditions properly. This is a part of ongoing work.

4 REINFORCEMENT CORROSION: MODELING

This section briefly describes analytical models adopted from the literature and further used in the numerical ex-

ample (Section 5), and the possible application of the experimental data presented in Section 2.2 to the utilized analytical models.

4.1 Analytical models

The formula for the penetration depth x (mm) at exposure time t (years) (time period after reinforcement depassivation) for the prediction of corrosion based on the application of Faraday's law reads (Rodriguez et al., 1996):

$$x = 0.0116\, i_{\text{corr}} t \qquad (6)$$

where i_{corr} is the value of the current density (μA/cm^2), which expresses the corrosion rate. The constant 0.0116 is a conversion factor from μA/cm^2 to mm/years under the assumptions that iron (Fe) has $n = 2$ (number of electrons freed by the corrosion reaction), $M = 55.85$ g/mol (molar mass), and $\rho = 7.88$ g/cm^3 (specific gravity).

The time-related net rebar diameter $d(t)$ can be estimated according to Rodriguez et al. (1996) as (see Figure 4a):

$$d(t) = d_i - x\, R_{\text{corr}} \qquad (7)$$

where d_i is the initial bar diameter (mm) and parameter R_{corr} [−] depends on the type of corrosion. Due to the assumed rotational symmetry in the case of uniform corrosion obviously $R_{\text{corr}} = 2$ (see Figure 4a). In the case of pitting corrosion R_{corr} represents a ratio between maximum and average corrosion penetration (i.e., the ratio between the rate of pitting and uniform corrosion penetration) and equals 4–8 according to Gonzales et al. (1995), although Darmawan and Stewart (2007) suggest $R_{\text{corr}} = 8$–11 and Tutti (1982) recommends $R_{\text{corr}} = 4$–10. The studies by Gonzalez et al. (1995) were performed on reinforcing steel embedded in concrete with a constant amount of chlorides added to the cement for both natural and accelerated conditions. Darmawan and Stewart (2007) performed accelerated tests on prestressed wires embedded in concrete with a constant amount of chlorides added to the cement. Tutti (1982) did not consider the effect of chlorides and used an external voltage source as a corrosion accelerator. However, all of the above-mentioned experimental work was performed without consideration of pH level and without exact consideration of different values of chloride concentration.

There is thus a very broad range of values for the parameter R_{corr}, and it is rather uncertain. From the geometrical point of view Equation (7) predicts a conservative value for net rebar diameter in the case of pitting corrosion (see Figure 4b). This simplification has been improved by Val and Melchers (1998), who considered
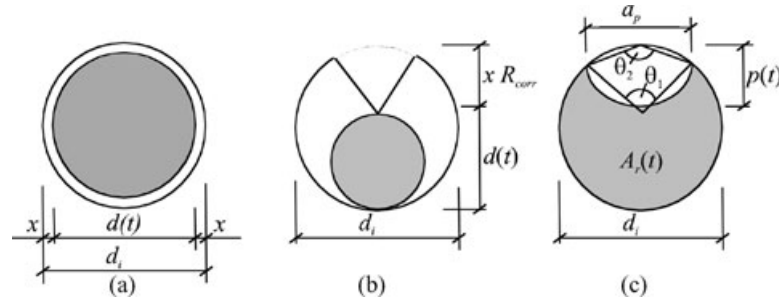
Fig. 4. The geometry of corroded steel rebar: (a) uniform corrosion (Rodriguez et al., 1996), (b) pitting corrosion (Rodriguez et al., 1996), and (c) pitting corrosion (Val and Melchers, 1998).

the hemispherical shape of the pit (see Figure 4c), where the pit depth p in time t is given as:

$$p(t) = x\, R_{\text{corr}}. \tag{8}$$

4.2 Effect of chloride concentration

The effect of chloride concentration near the reinforcement and other factors such as humidity, and pH level on corrosion rate penetration should be included in the parameter of i_{corr}. Let us mention a work by Engelund and Faber (2000), where they published the formula for electrical resistivity, which may be recalculated to i_{corr} according to the frequently used empirical expression (Alonso et al., 1988). They consider the effect of concrete curing, temperature, the presence of chlorides, and relative humidity via individual coefficients.

On the basis of our experiments presented in Section 2.2, the parameter i_{corr} was derived from the measurements as a function of chloride concentration C for two different pH values of 9 and 12.5 as depicted in Figure 5. It was recalculated from the corrosion rate found on the basis of experiments and rearranged on purpose to transform it into a uniform type of corrosion
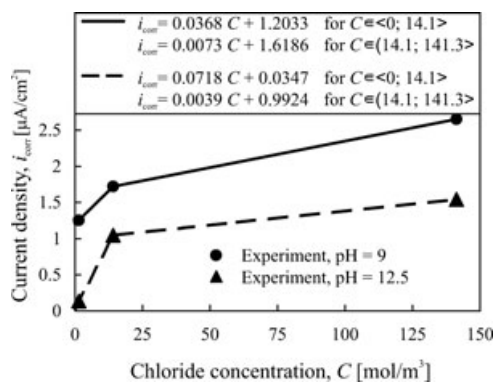
(Table 1) according to Equation (6). The pH values of 9 and 12.5 were chosen because the pH value of the pore solution is about 12.5 in the case of noncarbonated concrete and pH = 9 in the case of carbonated concrete. These values of i_{corr} are applied in an illustrative example in Section 5. Note that the proposed functions for i_{corr} may be applied for calculations of both the uniform (Equation 7) and pitting (Equation 7 or 8) types of corrosion; however, the coefficient R_{corr} for pitting corrosion has to be adopted from other sources as it was not determined in our experiments. By comparison of the method used in these experiments and the real conditions, our i_{corr} values are certainly somewhat on the safe side.

Note the current density i_{corr} is generally time dependent. However, for the sake of simplicity this has not been exploited in this article as already mentioned above. After all, it is frequently considered i_{corr} to be time independent (e.g., see Maruya et al., 2003, or Val et al., 2000). Moreover, the corrosion rate of steel in carbonated concrete decreases as the electrical resistivity increases, which is also not dealt with in this article; no universal correlation has been found yet (Bertolini, 2008). Partially, this uncertainty may be overcome by treating i_{corr} as a random variable. In addition, two different cases should be distinguished: (i) assessment of an existing structure where the results of possible measurements may be available and so the actual i_{corr} value may then be utilized for predictive modeling; (ii) the design of a new concrete structure under the consideration of durability, where our model may be exploited as a relatively simple variant for checking the design service life and/or for comparative purposes.

Fig. 5. The dependence of current density on chloride concentration.

5 NUMERICAL EXAMPLE

In the presented example a reinforced concrete rectangular cross section is exposed to chloride ingress simulated by the CA technique. To illustrate the
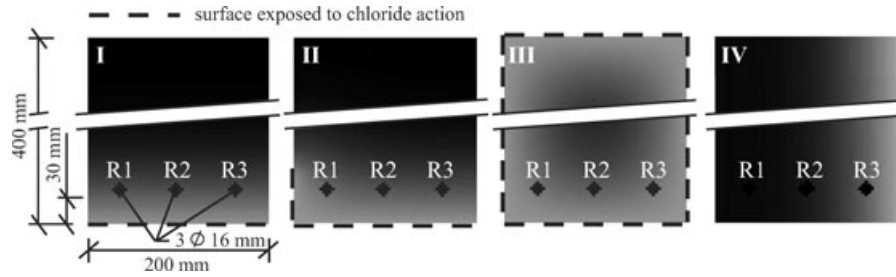
Fig. 6. Chloride ingress for four different boundary conditions (I, II, III, and IV). Cross-sectional area attacked by chloride are in gray and sections without chloride are black. Steel reinforcements are denoted R1, R2, and R3.

versatility of CA four different cases are assumed that differ in the surface areas exposed to chloride action as shown in Figure 6, together with their cross-section geometry. Surfaces bounded with a dashed line were supplied with chlorides in such a way that the surface concentration remained constant over the whole time period. The figure also documents the chloride distribution in the cross sections after 30 years of exposure. In case IV the seasonal chloride effect illustrated in Figure 3 was also applied.

The following input data for chloride diffusion simulation by CA were used: surface concentration of chlorides 60 mol/m^3 (in the case of seasonal effect this value corresponds to the maximum concentrations), cell size 0.0032 m, time step 7.402 days, diffusion coefficient 2×10^{-12} m^2/second, and evolution coefficients 0.5 and 0.125 for central and surrounding cells, respectively. As already mentioned above, the "reflecting boundary" rule was applied in this example. The developments of chloride concentrations over time in the vicinity of steel reinforcements R1, R2, and R3 are plotted in Figure 7. Figure 7a compares the chloride ingress

evolution for boundary conditions I–IV with a constant surface concentration (CC), and Figure 7b shows the difference between constant surface concentration and seasonal effect (SE) for boundary condition IV. The chloride concentration in the individual time steps is determined as an average concentration from the cells representing concrete that bounds the steel cells. Due to certain symmetries in boundary conditions some of the rebars are attacked identically.

When we apply Equation (7) using $R_{corr} = 2$ (uniform corrosion), $d_i = 16$ mm, and the function for i_{corr} in Figure 5 (namely pH = 12.5 pointing to noncarbonated concrete), we obtain a drop in the rebars' diameters over time due to corrosion. The results of the analysis are plotted in Figure 8a for boundary conditions IV (R1–R3) and III (R1 and R3). Both CC and SE conditions are compared for boundary type IV. Note that the rebars R1, R3_III, and R1_IV are the ones with the highest and the lowest chloride concentrations, respectively, as seen in Figure 7a. Let us assume random input parameters and perform a probabilistic computation for rebar R3_IV (CC) using FReET-D software
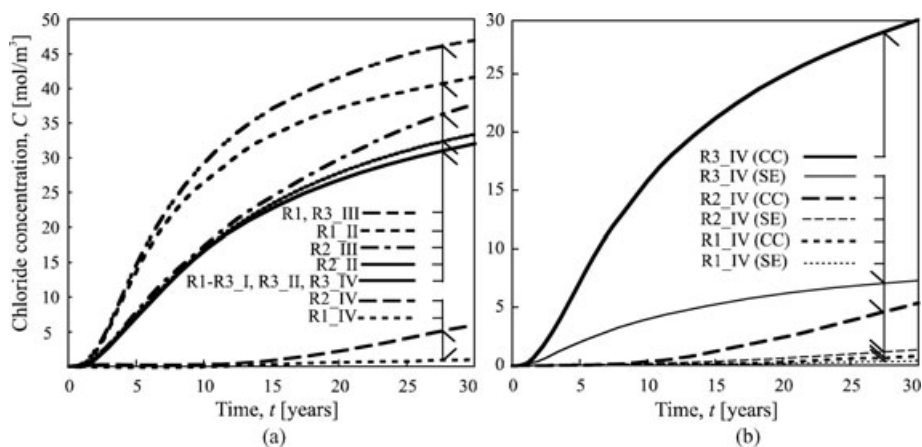
Fig. 7. Development of chloride concentration in the vicinity of the steel rebars: (a) constant surface chloride concentration for boundary conditions I–IV and (b) comparison of constant surface chloride concentration (CC) and seasonal effect (SE) for boundary condition IV.
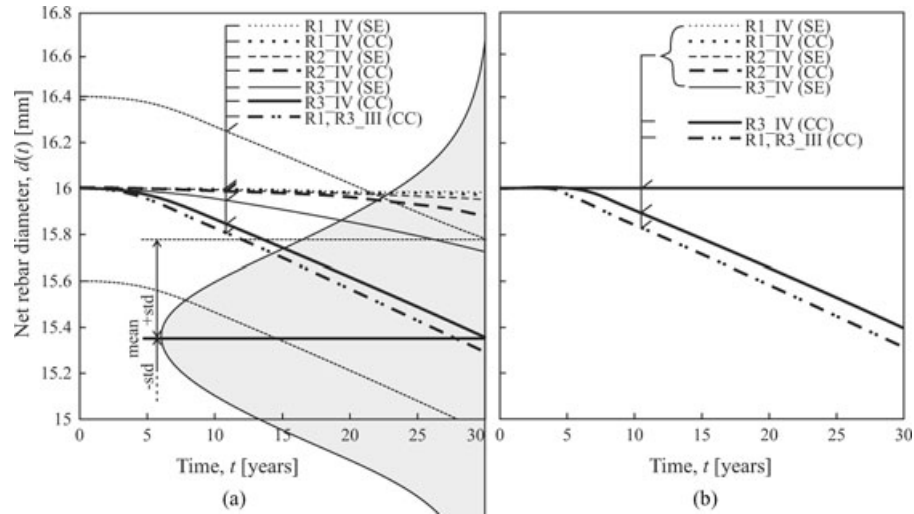
Fig. 8. The drop in rebars' diameters over time due to corrosion for boundary conditions III and IV: (a) without and (b) with the assumption of critical chloride concentration according to Papadakis et al. (1996).

(Teplý et al., 2007) with the following input parameters: initial rebar diameter d_i is lognormal (2 par) with a mean of 16 mm and a coefficient of variation (COV) of 2.5%; current density i_{corr} is normal with a mean given by Figure 5 and COV 20%, coefficient $R_{corr} = 2$, and is deterministic.

The results of this probabilistic analysis are depicted in Figure 8a by a PDF curve of the resulting rebar diameter at time $t = 30$ years gained by means of the best fit (beta PDF with mean = 15.35 mm and the standard deviation = 0.42 mm), thus showing the possible scatter. For the generation of sample sets from the input variables the LHS method was applied in this example. Sample size was 1,000.

According to various authors (Glass and Buenfeld, 1995, 1997; Duprat, 2007; Ann and Song, 2007), the corrosion of steel embedded in concrete starts to propagate at a certain level of chloride concentration called critical concentration depending also on other factors such as pH level. Let us apply for pH = 12.5 a critical concentration of 9.48 mol/m^3, which corresponds to a Cl$^-$/OH$^-$ ratio of 0.3, considered as a signal for steel depassivation due to chlorides recommended by Papadakis et al. (1996). The results of the deterministic analysis performed with the assumption of zero corrosion penetration if the chloride concentration in the vicinity of steel rebar is lower to the critical one are plotted in Figure 8b. By comparison of both Figures 8a and b it is evident that the differences for R3_IV (CC) and R1, R3_III (CC) at $t = 30$ years are quite negligible; they are 0.25 and 0.14%, respectively. The other rebars in Figure 8b did not reach the assumed critical chloride concentration (compare in Figure 7) in the an-

alyzed time interval, thus corrosion had not yet been initiated.

To continue this study let us construct a probability condition:

$$P_f = P\left[A_{R1}(t) + A_{R2}(t) + A_{R3}(t) \leq A_{cr}\right] \quad (9)$$

where P_f is the probability of failure, A_{cr} is the critical area of steel in the whole cross section (e.g., leading to the exceeding of SLS or ULS) and $A_{R1}(t)$, $A_{R2}(t)$, and $A_{R3}(t)$ are the areas of steels R1_IV, R2_IV, and R3_IV, respectively, at time t. We assume that A_{cr} is 90% of the initial rebars' areas in the concrete cross section, and that it is deterministic. The other inputs are considered to be random (except to R_{corr}) and have already been given above. The critical chloride concentration is not considered. Again utilizing the FReET-D module we arrive at P_f and corresponding reliability coefficients β for the chosen time steps—see Table 2 for both CC and SE types of chloride supply. The values of P_f and β were obtained by the FORM method. As expected, the SE case affords a safer prognosis. It must be noted

Table 2
The results of the probability condition (9)

Time (years)	30	20	10	5
		CC		
P_f [−]	0.0795	0.0436	0.0248	0.0195
β	1.41	1.71	1.96	2.06
		SE		
P_f [−]	0.0366	0.0264	0.0205	0.0188
β	1.79	1.94	2.04	2.08

that the limit condition (9) does not consider any particular structure with mechanical load and the results of this study may serve for the probabilistic prediction of the time of reaching certain reinforcement corrosion limits only; β describes in this case the reliability level of critical corrosion or of the service life based on such a limit. Such a limit is obviously governed by the structure's configuration, loading, and the limit state in question, that is, SLS, ULS, or DLS (e.g., the consideration of cracks in concrete due to reinforcement corrosion during the propagation period—see Teplý et al., 2007).

6 CONCLUSIONS AND IMPLICATIONS IN PRACTICE

1. The present article concentrates on the assessment of chloride concentration fields by numerical methods, modeling of reinforcement corrosion, and on their practical utilization while evaluating the limit states, service lives, and relevant reliability of reinforced concrete structures.

2. The current trend for the durability assessment of concrete structures is the probabilistic performance-based approach; it is presented in this article with the focus on chloride impact.

3. The effects of chloride presence manifest themselves (i) during the initiation period—the field of chloride concentration within the concrete structure modeled as a diffusion process is determined with special emphasis on the critical value necessary for initiation limit state and relevant service life assessment; (ii) during the propagation period, that is, after the commencement of rebar corrosion.

4. The development of the concentration of chlorides over time and within the cross section of an RC structure is modeled by a specific CA technique while deterministic and stochastic options are encompassed in a software tool. This may serve effectively in practice, for example, for simulating the degradation of concrete structures due to seasonal de-icing salt application, and for consideration of the time and space dependency of chloride permeability.

5. The presented experimental work shows the effect of chloride concentration and pH values on the rate of steel corrosion. The results of the CA technique and the laboratory experiments are applied in the assessment of steel corrosion by means of a randomized analytical model where the value of i_{corr} is considered to be influenced by Cl^- concentration and pH values.

6. CA technique is more feasible and versatile concerning the easiness in handling time- or space-dependant external effects and diffusive quality of concrete. The process is transparent and no equation sets have to be solved.

7. The introduced approach is applied to an illustrative example showing the effect of chloride concentration level at different points in a cross section of an RC structure on the rate of steel corrosion over time for different "loading" situations. In this manner an arbitrary location (represented by a longitudinal or cross section) in an RC structure may be analyzed.

8. The combination of a 2D CA technique and probabilistic 1D modeling of concrete degradation is a new and effective way of assessing the initiation and/or propagation period of the deterioration of a concrete structure. It creates the feasibility of more complex design/assessment of RC structures, utilizing statistical and reliability analyses of durability, serviceability, and ultimate limit states (considering both the initial and propagation periods) in the context of current trends represented in international documents (*fib* Model Code and ISO 13823). The presented approach supports design procedures accommodating possible corrosion of RC structures and may help to reduce heavy repair costs in the future.

REFERENCES

Alonso, C., Andrade, C. & Gonzáles, J. A. (1988), Relation between resistivity and corrosion rate of reinforcements in carbonated mortar made with several cement types, *Cement and Concrete Research*, **8**(5), 687–98.

Ann, K.Y. & Song, H. W. (2007), Chloride threshold level for corrosion of steel in concrete, *Corrosion Science*, **49**, 4113–33.

Bentur, A., Diamond, S. & Berke, N. S. (1997), *Steel Corrosion in Concrete*, Taylor and Francis Group, London and New York.

Bertolini, L. (2008), Steel corrosion and service life of reinforced concrete structures, *Structure and Infrastructure Engineering*, **4**(2), 123–37.

Biondini, F., Bontempi, F., Frangopol, D. M. & Malerba, P. G. (2004), Cellular automata approach to durability analysis of concrete structures in aggressive environments, *Journal of Structural Engineering ASCE*, **130**(11), 1724–37.

Bird, H. E. H., Pearson, B. R. & Brook, P. A. (1988), The breakdown of passive film on iron, *Corrosion Science*, **28**(1), 81–86.

Bogard, B., Warren, C., Somayaji, S. & Heidersbach, R. (1990), *Mechanism of Corrosion of Steel in Concrete*, Corrosion Rates of Steel in Concrete, ASTM STP 1065, American Society for Testing and Materials, Philadelphia, 174–88.

Collepardi, M., Marcialis, A. & Turriziani, R. (1972), Penetration of chloride ions into cement pastes and concrete, *Journal of American Ceramic Society*, **55**(10), 534–35.

Costa, A. & Appleton, J. (1999), Chloride penetration into concrete in marine environments—Part II: prediction of long term chloride penetration, *Materials and Structures*, **32**, 354–59.

ČSN 425535, Tyče žebírkové pro výztuž do betonu z oceli značky 10 425. Rozměry (High-bond bars for concrete reinforcement made of steel 10 425. Dimensions.) Validity: 12/1978–12/2007 (in Czech).

Darmawan, M. S. & Stewart, M. G. (2007), Effect of pitting corrosion on capacity of prestressing wires, *Magazine of Concrete Research*, **59**(2), 131–39.

Duprat, F. (2007), Reliability of RC beams under chloride-ingress, *Construction and Building Materials*, **21**, 1605–16.

DuraCrete. (1998) BE95-1347, Summary of the statistical quantification of the DuraCrete resistivity corrosion rate model, prepared by ibac, Institute for Building and Construction Research, Technical University of Aachen, Germany, and Chalmers University of Technology, Sweden.

EN 1990 (2002), Basis of structural design, Eurocode 0, CEN, 2002.

EN 1992-1-1 (2003), Design of concrete structures—Part 1.1: general rules and rules for building, Eurocode 2, CEN, 2003.

Engelund, S. & Faber, M. H. (2000), Development of a code for durability design of concrete structures, in R. E. Melchers and M. G. Stewart (eds.), *Applications of Statistics and Probability*, Balkema, Rotterdam, ISBN 90 5809 086 8.

fib Model Code (2006), Bulletin No. 34, Service Life Design, part of the future *fib* Model Code 2010.

Glass, G. K. & Buenfeld, N. R. (1995), Chloride threshold levels for corrosion induced deterioration of steel in concrete, in O. Nilsson and J. P. Ollivier (eds.), in *Proc. of the International Workshop Chloride Penetration into Concrete, RILEM Publications*, Vol. 1, St. Rémy-les-Cheuvreuse, France, 429–39.

Glass, G. K. & Buenfeld, N. R. (1997), The presentation of the chloride threshold level for corrosion of steel in concrete, *Corrosion Science*, **39**(5), 1001–13.

Gonzales, J. A., Andrade, C., Alonso, C. & Feliu, S. (1995), Comparison of rates of general corrosion and maximum pitting penetration on concrete embedded steel reinforcement, *Cement and Concrete Research*, **25**(2), 257–64.

Hunkeler, F. (2005), Corrosion in reinforced concrete: processes and mechanisms, in H. Bőhni (ed.), in *Proc. of Corrosion in Reinforced Concrete Structures*, Woodhead Publishing Limited, Cambridge.

ISO 2394 (1998), General principles on reliability for structures, ISO.

ISO 13823 (2008), General principles in the design of structures for durability.

Jensen, O. M., Hansen, P. F., Coats, A. M. & Glasser, F. P. (1999), Chloride ingress in cement paste and mortar, *Cement and Concrete Research*, **29**, 1497–1504.

Karimi, A. R. & Ramachandran, K. (2000), Probabilistic estimation of corrosion in bridges due to chlorination, in R. E. Melchers and M. G. Stewart (eds.), *Applications of Statistics and Probability*, Balkema, Rotterdam.

Mangat, P. S. & Molloy, B. T. (1994), Predicting of long-term chloride concentration in concrete, *Materials and Structures*, **27**(170), 338–46.

Maruya, T., Hsu, K., Takeda, H. & Tangtermisikirul, S. (2003), Numerical modeling of steel corrosion in concrete structures due to chloride ion, oxygen and water movement, *Journal of Advanced Concrete Technology*, **1**(2), 147–60.

Montemor, M. F., Simoes, A. M. P. & Ferreira, M. G. S. (2003), Chloride-induced corrosion on reinforcement steel: from the fundamental to the monitoring techniques, *Cement and Concrete Research*, **25**, 491–502.

Nguyen, T. S., Lorente, S. & Carcasses, M. (2006), Influence of temperature on chloride transport through cementitious materials, *Journal de Physique IV*, **136**, 63–70.

Nilsson, L. O. (2006), Present limitations of models for predicting chloride ingress into reinforced concrete structures, *Journal de Physique IV*, **136**, 123–30.

Nürnberger, U. (1984), Chloride corrosion of steel in concrete, Betonwerk – Fertigteil Technik, Part 1, 9, 601–612; Part 2, 10, 697–704.

Papadakis, V. G., Roumeliotis, A. P., Fardis, C. G. & Vagenas, C. G. (1996), Mathematical modeling of chloride effect on concrete durability and protection measures, in R. K. Dhir and M. R. Jones (eds.), in *Proc. of International Conference on Concrete in the Service of Mankind (Concrete Repair, Rehabilitation and Protection)*, Dundee, Scotland, UK, 165–74.

Podroužek, J., Teplý, B. & Chromá, M. (2008), Modeling of chloride ion ingress: temporal and spatial variation, in Bílek and Keršner (eds.), in *Proc. of 3rd International Symposium Non-Traditional Cement and Concrete Composites*, Brno, Czech Republic, 570–77.

RILEM Report 14 (1996), *Durability Design of Concrete Structures*, in A. Sarja and E. Vesikari (eds.), E & FN SPON, London, 165 p.

Rodriguez, J., Ortega, L. M., Casal, J. & Diez, J. M. (1996), Corrosion of reinforcement and service life of concrete structures, in *Proc. of Int. Conf. on Durability of Building Materials and Components 7*, Vol. 1, Stockholm, pp. 117–26.

Schueremans, L., Gemert, D. V. & Giessler, S. (2007), Chloride penetration in RC-structures in marine environments—long-term assessment of a preventive hydrophobic treatment, *Construction and Building Materials*, **21**, 1238–49.

So, H. S. & Millard, S. G. (2007), On-site measurements of corrosion rate of steel in reinforced concrete, *ACI Material Journal*, **104**(6), 638–42.

Stewart, M. G. & Rosowsky, D. (1998), Structural safety and serviceability of concrete bridges subject to corrosion, *Journal of Infrastructure Systems*, **4**(4), 146–54.

Tang, L. (2007), Service-life prediction based on the rapid migration test and the ClinConc model, in *Proc. of International RILEM Workshop on Performance Based Evaluation and Indicators for Concrete Durability*, 19–21 March 2006, Madrid, Spain, 157–64.

Tang, L. & Gulikers, J. (2007), On the mathematics of time-dependent apparent chloride diffusion coefficient in concrete, *Cement and Concrete Research*, **37**(4), 589–95.

Tang, L. & Nilsson, L. O. (1992), Chloride diffusivity in high strength concrete at different ages, *Nordic Concrete Research*, **11**, 162–71.

Teplý, B., Matesová, D., Chromá, M. & Rovnaník, P. (2007), Stochastic degradation models for durability limit state evaluation: SARA—Part VI, in *Proc. of 3rd International Conference on Structural Health Monitoring of Intelligent Infrastructure (SHMII-3 2007)*, Vancouver, Canada, 187.

Thomas, M. D. A. & Bamforth, P. B. (1999), Modeling chloride diffusion in concrete: effect of fly ash and slag, *Cement and Concrete Research*, **29**, 487–95.

Tikalsky, P. J. (2005), Monte Carlo simulation of chloride diffusion in concrete exposed to de-icing salts, in R. K. Dhir, M. J. McCarthy, and S. Caliskan (eds), *6th International Congress Global Construction: Ultimate Concrete Opportunities (Concrete for Transportation Infrastructure)*, Dundee, Scotland, UK, pp. 251–58.

Tutti, K. (1982), *Corrosion of Steel in Concrete*, Swedish Cement and Concrete Research Institute, Stockholm, Sweden.

Val, D. & Melchers, R. E. (1998), Reliability analysis of deteriorating reinforced concrete frame structures, *Structural Safety and Reliability*, Vol 1, Balkema, Rotterdam, pp. 105–12.

Val, D., Stewart, G. M. & Melchers, R. E. (2000), Life-cycle performance of RC bridges: probabilistic approach, *Computer-Aided Civil and Infrastructure Engineering*, **15**, 14–25.

Wolfram, S. (1994), *Cellular Automata and Complexity—Collected Papers*, Addison-Wesley.

Xi, Y. & Bažant, P. B. (1999), Modeling chloride penetration in saturated concrete, *ASCE Journal of Materials in Civil Engineering*, **11**(1), 58–65.